Dynamics of Thermal Effects in the Spin-Wave Theory of Quantum Antiferromagnets

Ángel Rivas and Miguel A. Martin-Delgado
Departamento de Física Teórica I, Facultad de Ciencias Físicas, Universidad Complutense, 28040 Madrid, Spain

We derive a master equation which allows us to study non-equilibrium dynamics of a quantum antiferromagnet. By resorting to spin wave theory we obtain a closed analytic form for the magnon decay rates. These turn out to be closely related to form factors, which are experimentally accessible by means of neutron and Raman scattering. Furthermore, we compute the time-evolution of the staggered magnetization showing that, for moderate temperatures, the magnetic order is not spoilt even if the coupling is fully isotropic.

PACS numbers: 42.50.Lc, 03.65.Yz, 75.30.Ds, 75.10.Jm

I. INTRODUCTION

The properties of the quantum Heisenberg model play a fundamental role in the physics of many-body effects for models defined by quantum Hamiltonians on a lattice, in several spatial dimensions [1, 2]. One of the first non-perturbative methods devised to study the quantum Heisenberg model is known as spin-wave theory (SWT). This is a type of mean-field theory method that is specially suited to study the quantum fluctuations of interacting spins. The basic assumption is the existence of a ground state that spontaneously breaks the global symmetry of the Heisenberg Hamiltonian. In this case, it corresponds to rotational symmetry SO(3) about an arbitrary axis. In SWT this symmetry is broken by fixing a preferred axis called magnetization axis of the ground state, and excitations appear in the form of fluctuations from the fixed direction. These are the Goldstone bosons of this spontaneously breaking mechanism and represent the magnon modes propagating as spin waves in the quantum system. However, spatial dimensionality is crucial in order to have a well-defined semiclassical expansion in the parameter $1/S$, where S is the total spin at each site of the system lattice. Namely, in a quantum antiferromagnet the spatial dimension of the lattice has to be large enough in order to sustain the assumption of a given order in the ground state. Otherwise, strong quantum fluctuations in one-dimensional lattices break the long range order and makes the SWT invalid. However, many interesting systems are materials in 3D and SWT provides very good approximations to their observable quantities.

SWT has been extensively developed in many aspects. It has become by now an standard and reference tool in order to have a good approximate description of quantum antiferromagnetic systems, whenever the validity of its application is justified.

To the best of our knowledge, there is an important aspect of SWT that remains vaguely explored. Namely, the modification of SWT in order to adapt it to describe the natural interaction of a quantum antiferromagnet with an external or surrounding thermal bath that is interacting with it. A typical example is provided by the phonons of the lattice where the quantum spins are located. This is a basic and fundamental problem since it entails the description of both dynamical effects, i.e. time-dependent, as well as finite temperature effects outside the state of thermal equilibrium.

Embedding thermal fluctuations in the dynamics of a system may be approached from several points of view. For instance, in the classical domain it is common to consider the effect of a noisy magnetic thermal field acting on the Heisenberg Hamiltonian [3]. However, that situation is different from what we focus in this work, where the noise is described from a microscopic model based on thermal excitation of the surrounding environment. The branch of the quantum theory which deals with this kind of problems is the theory of open quantum systems [4–7] that plays a fundamental role in quantum information theory [8, 9]. From this point of view, the quantum magnet is considered as an open system, which exchanges energy with its environment.

The best method to describe an open system strongly depends on the explicit nature of each situation. In this work we have applied the Davies formalism, which is a suitable description of an open system weakly interacting with a large environment. One its main features is that it allows us to derive an evolution equation for any spin observable of the quantum antiferromagnet coupled to a generic thermal bath at a certain temperature T. Namely, it provides us with an equation for the evolution of density matrix $\rho(t)$. Furthermore, as a consequence of how this fundamental equation is obtained, a series of interesting results for the enlarged SWT have being obtained: i/ the quantum antiferromagnet thermalizes towards the Gibbs state for long enough times; ii/ the decay rate of this thermalization process can be obtained in closed analytical form as a function of the lattice momentum; iii/ the thermal bath cannot be arbitrary in order to ensure the convergence of any observable to its thermal value, but it has to belong to the class of super-ohmic baths with specific parameters depending on the quantum antiferromagnet; iv/ the staggered magnetization can be computed analytically and we can obtain its behaviour with time and temperature thereby unveiling the fate of the antiferromagnetic order parameter and v/ the thermal evolution of the magnon form factor can be also computed explicitly. These quantities are of physical

importance and observable in inelastic neutron scattering experiments [10–12], Raman experiments [13] etc.

This paper is organized as follows: in Sect.II we review the linear spin-wave theory and establish our notation. Sect.III describes the microscopic coupling of the SWT Hamiltonian with a Hamitonian bath of bosonic operators. In Sect.IV we derive the complete master equation for describing the evolution and thermal effects of the whole interacting system-bath. In Sect.V we compute relevant observables under the above conditions, such as the staggered magnetization, two-spin correlators and form factors. Sect.VI is devoted to conclusions. We refer to appendix A for expressions of the time-evolution of the first and second moments, and to appendix B for the detailed calculation involving the two-spin spatial correlation functions.

II. SPIN WAVE THEORY FOR QUANTUM ANTIFERROMAGNETS

First of all, let us briefly remind the spin wave theory for quantum antiferromagnets and to establish our notation. The system consists of a lattice with a spin S on every vertex. The Hamiltonian contains only two-body terms between first neighbors according to a Heisenberg interaction

$$H_S = J \sum_{\langle \boldsymbol{r},\boldsymbol{r}'\rangle} \boldsymbol{S}_{\boldsymbol{r}} \cdot \boldsymbol{S}_{\boldsymbol{r}'}, \tag{1}$$

with $J > 0$ for antiferromagnetism. The phenomenology displayed by this Hamiltonian strongly depends on the morphology of the lattice. Particularly if the lattice is bipartite (i.e. we can define two sublattices A and B in such a way that the first neighbours of a A belong to B and viceversa, see figure 1) the ground state is close to a staggered spin configuration known as Néel state. However if the lattice is not bipartite (e.g. triangular lattice) the system becomes frustrated, and no simple configuration is found to be a ground state for the diagonal part of the Hamiltonian (1). For our purposes we shall consider a square lattice.

The diagonalization of the Hamiltonian (1) is not an easy task, and no exact solutions are known for spatial dimensions $d \geq 2$, or for spins $S \geq 1$ in $d = 1$. Thus, approximation methods become very useful. Probably the most fundamental of them is based on the Holstein–Primakoff approximation [14, 15] and leads to the so-called spin wave theory [16], which is also applicable to ferromagnets [17]. This method rewrites the spin operators in terms of bosonic annihilation and creation operators, a and $a^\dagger$, $[a, a^\dagger] = 1$. Concretely, for $\boldsymbol{r}$ in the sublattice A

$$\begin{aligned} S^+_{\boldsymbol{r}} &= \sqrt{2S} f_S(a^\dagger_{\boldsymbol{r}} a_{\boldsymbol{r}}) a_{\boldsymbol{r}}, \\ S^-_{\boldsymbol{r}} &= \sqrt{2S} a^\dagger_{\boldsymbol{r}} f_S(a^\dagger_{\boldsymbol{r}} a_{\boldsymbol{r}}), \\ S^z_{\boldsymbol{r}} &= S - a^\dagger_{\boldsymbol{r}} a_{\boldsymbol{r}}, \end{aligned} \tag{2}$$

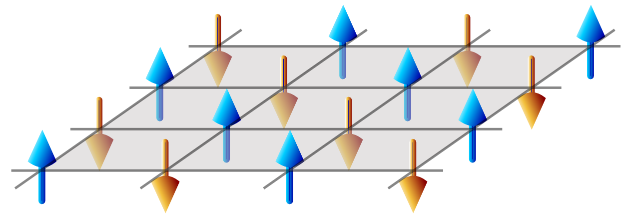

FIG. 1: Arrange of a quantum antiferromagnet in the Néel state on a square lattice. The color of the spins denotes the two different sublattices, A (blue arrows) and B (orange arrows). The true ground state is close to this staggered configuration, however there is a slight disarrange in the orientation of the spins due to quantum fluctuations.

and for $\boldsymbol{r}$ in the sublattice B

$$\begin{aligned} S^+_{\boldsymbol{r}} &= \sqrt{2S} b^\dagger_{\boldsymbol{r}} f_S(b^\dagger_{\boldsymbol{r}} b_{\boldsymbol{r}}), \\ S^-_{\boldsymbol{r}} &= \sqrt{2S} f_S(b^\dagger_{\boldsymbol{r}} b_{\boldsymbol{r}}) b_{\boldsymbol{r}}, \\ S^z_{\boldsymbol{r}} &= b^\dagger_{\boldsymbol{r}} b_{\boldsymbol{r}} - S, \end{aligned} \tag{3}$$

with

$$f_S(x) = \left(1 - \frac{x}{2S}\right)^{1/2}. \tag{4}$$

By writing the Hamiltonian (1) at first order in $f_S(x)$ we obtain the so-called linear spin-wave theory:

$$\begin{aligned} H_{LSW} = \; & J \left[-NdS^2 + 2dS \textstyle\sum_{\boldsymbol{r}} (a^\dagger_{\boldsymbol{r}} a_{\boldsymbol{r}} + b^\dagger_{\boldsymbol{r}} b_{\boldsymbol{r}}) \right. \\ & \left. + S \textstyle\sum_{\langle \boldsymbol{r},\boldsymbol{r}'\rangle} (a_{\boldsymbol{r}} b_{\boldsymbol{r}'} + a^\dagger_{\boldsymbol{r}} b^\dagger_{\boldsymbol{r}'}) \right]. \end{aligned} \tag{5}$$

This approximation is valid to describe states where $\langle f_S(a^\dagger_{\boldsymbol{r}} a_{\boldsymbol{r}})\rangle = \langle f_S(b^\dagger_{\boldsymbol{r}} b_{\boldsymbol{r}})\rangle \simeq 1$, and thus they also verify

$$\langle a^\dagger_{\boldsymbol{r}} a_{\boldsymbol{r}}\rangle, \; \langle b^\dagger_{\boldsymbol{r}} b_{\boldsymbol{r}}\rangle \ll 2S. \tag{6}$$

This is the self-consistent condition characteristic of this mean-field theory method.

The Hamiltonian H_{LSW} is quadratic in boson operators, so in order to diagonalize it we take Fourier transform

$$a_{\boldsymbol{r}} = \sqrt{\frac{1}{N_A}} \sum_{\boldsymbol{k}} \mathrm{e}^{-\mathrm{i}\boldsymbol{k}\cdot\boldsymbol{r}} a_{\boldsymbol{k}}, \tag{7}$$

$$b_{\boldsymbol{r}} = \sqrt{\frac{1}{N_B}} \sum_{\boldsymbol{k}} \mathrm{e}^{\mathrm{i}\boldsymbol{k}\cdot\boldsymbol{r}} b_{\boldsymbol{k}}, \tag{8}$$

with $N_A = N_B = N/2$ for a square lattice and the lattice wave vector takes on the following discretized values,

$$\boldsymbol{k} = \frac{2\pi \boldsymbol{m}}{N_{A,B}} = \frac{4\pi \boldsymbol{m}}{N}, \;\; \boldsymbol{m} \in A, B. \tag{9}$$

Then the first term of H_{LSW} is easy to compute given the orthonormalization rule $\frac{2}{N}\sum_{\boldsymbol{r}\in A,B} \mathrm{e}^{\mathrm{i}\boldsymbol{k}\cdot\boldsymbol{r}} = \delta_{\boldsymbol{k},0}$. For the second one, we parameterize $\boldsymbol{r}'$ neighbour to $\boldsymbol{r}$ as

$\boldsymbol{r}' = \boldsymbol{r} + \hat{\boldsymbol{r}}_\mu$, where $\hat{\boldsymbol{r}}_\mu$ is the unit vector in the μ direction, which in $d = 3$ and starting from the first site, can be $(1,0,0)$, $(0,1,0)$ or $(0,0,1)$. Thus we obtain

$$H_{LSW} = J\Big[-NdS^2 + 2S\sum_{\boldsymbol{k}} d(a^\dagger_{\boldsymbol{k}}a_{\boldsymbol{k}} + b^\dagger_{\boldsymbol{k}}b_{\boldsymbol{k}}) + \xi_{\boldsymbol{k}}(a_{\boldsymbol{k}}b_{\boldsymbol{k}} + a^\dagger_{\boldsymbol{k}}b^\dagger_{\boldsymbol{k}})\Big], \quad (10)$$

where

$$\xi_{\boldsymbol{k}} = \sum_\mu \cos(\boldsymbol{k}\cdot\hat{\boldsymbol{r}}_\mu).$$

Next step is to perform a Bogoliubov transformation to new boson operators $\alpha_{\boldsymbol{k}}$ and $\beta_{\boldsymbol{k}}$,

$$a_{\boldsymbol{k}} = \cosh(\theta_{\boldsymbol{k}})\alpha_{\boldsymbol{k}} - \sinh(\theta_{\boldsymbol{k}})\beta^\dagger_{\boldsymbol{k}}, \quad (11)$$

$$b_{\boldsymbol{k}} = -\sinh(\theta_{\boldsymbol{k}})\alpha^\dagger_{\boldsymbol{k}} + \cosh(\theta_{\boldsymbol{k}})\beta_{\boldsymbol{k}}. \quad (12)$$

The function $\theta_{\boldsymbol{k}}$ is chosen so that the coefficient of $\alpha_{\boldsymbol{k}}\beta_{\boldsymbol{k}}$ and $\alpha^\dagger_{\boldsymbol{k}}\beta^\dagger_{\boldsymbol{k}}$ is zero:

$$\tanh(2\theta_{\boldsymbol{k}}) = \frac{\xi_{\boldsymbol{k}}}{d}. \quad (13)$$

With this choice the Hamiltonian of the system is diagonalized

$$H_{LSW} = E_0^0 + \sum_{\boldsymbol{k}} \omega(\boldsymbol{k})(\alpha^\dagger_{\boldsymbol{k}}\alpha_{\boldsymbol{k}} + \beta^\dagger_{\boldsymbol{k}}\beta_{\boldsymbol{k}}). \quad (14)$$

Here the energy dispersion relation is

$$\omega(\boldsymbol{k}) = 2JS\sqrt{d^2 - \xi^2_{\boldsymbol{k}}}, \quad (15)$$

and E_0^0 is a constant

$$E_0^0 = -JNS\left[dS + \frac{2}{N}\sum_{\boldsymbol{k}}\left(d - \sqrt{d^2 - \xi^2_{\boldsymbol{k}}}\right)\right].$$

In summary, we have transformed the intricate Hamiltonian (1) with interaction terms into another approximate Hamiltonian which is just a collection of uncoupled harmonic oscillators, and so it is easy to write the whole spectrum analytically. The excitation of these harmonic oscillators are called "magnons", because they represent the minimal collective magnetic excitation of the spin lattice.

III. INTERACTION WITH A BOSONIC ENVIRONMENT

The antiferromagnetic system may be affected by a dissipative dynamics due to the interaction with its environment. In principle the most common source of dissipation will be phonon excitations in the lattice. Thus, the interaction Hamiltonian will be given typically by the so-called spin-boson model [5, 18]

$$V = \sum_j \sum_{\boldsymbol{r}} g(\omega_j)(S^x_{\boldsymbol{r}} + S^y_{\boldsymbol{r}} + S^z_{\boldsymbol{r}})(A_{\boldsymbol{r},j} + A^\dagger_{\boldsymbol{r},j}), \quad (16)$$

where A and $A^\dagger$ are the annihilation and creation operators of the environmental boson modes (which are considered to be local), and we have assumed that the coupling function $g(\omega_j)$ is isotropic and the same for every member of the lattice. In addition, the Hamiltonian of the environment is

$$H_E = \sum_j \sum_{\boldsymbol{r}} \omega_j A^\dagger_{\boldsymbol{r},j}A_{\boldsymbol{r},j}, \quad (17)$$

which is written as

$$H_E = \sum_j \sum_{\boldsymbol{k}} \omega_j A^\dagger_{\boldsymbol{k},j}A_{\boldsymbol{k},j}, \quad (18)$$

after taking Fourier transform.

In linear spin wave theory approximation, the interaction term reads

$$V_{LSW} = \sum_j\sum_{\boldsymbol{r}} g(\omega_j)\Big[(1-\mathrm{i})\sqrt{\tfrac{S}{2}}(a_{\boldsymbol{r}} + b^\dagger_{\boldsymbol{r}}) + (1+\mathrm{i})\sqrt{\tfrac{S}{2}}(a^\dagger_{\boldsymbol{r}} + b_{\boldsymbol{r}}) + 2S - (a^\dagger_{\boldsymbol{r}}a_{\boldsymbol{r}} - b^\dagger_{\boldsymbol{r}}b_{\boldsymbol{r}})\Big](A_{\boldsymbol{r},j} + A^\dagger_{\boldsymbol{r},j}).$$

Now the whole Hamiltonian has become much more involved than the original spin-wave theory Hamiltonian. However, we can consider a simplified version of this Hamiltonian based on the following facts,

- We ignore the term $2S(A_{\boldsymbol{r},j} + A^\dagger_{\boldsymbol{r},j})$ because it commutes with all observables of the system, which are the only interesting for us, as we going to trace out the environment later.
- The terms $a^\dagger_{\boldsymbol{r}}a_{\boldsymbol{r}}$ and $b^\dagger_{\boldsymbol{r}}b_{\boldsymbol{r}}$ are negligible in comparison to the others in the regime where the spin wave theory is valid (6).
- Since $|(1\pm\mathrm{i})/\sqrt{2}| = 1$, we have taken all the coefficients of $a_{\boldsymbol{r}}$, $a^\dagger_{\boldsymbol{r}}$, $b_{\boldsymbol{r}}$, $b^\dagger_{\boldsymbol{r}}$ to be just $\sqrt{S}$. This is not really a substantial modification to the dynamics but simplifies subsequent computations.

Therefore, we arrive at

$$V_{LSW} = \sqrt{S}\sum_j\sum_{\boldsymbol{r}} g(\omega_j)\left(a_{\boldsymbol{r}} + b^\dagger_{\boldsymbol{r}} + a^\dagger_{\boldsymbol{r}} + b_{\boldsymbol{r}}\right)(A_{\boldsymbol{r},j} + A^\dagger_{\boldsymbol{r},j}), \quad (19)$$

and by taking Fourier transform this interaction becomes

$$V_{LSW} = \sqrt{S}\sum_j\sum_{\boldsymbol{k}} g(\omega_j)\Big[(a_{\boldsymbol{k}} + b^\dagger_{\boldsymbol{k}})(A_{-\boldsymbol{k},j} + A^\dagger_{\boldsymbol{k},j}) + (a^\dagger_{\boldsymbol{k}} + b_{\boldsymbol{k}})(A_{\boldsymbol{k},j} + A^\dagger_{-\boldsymbol{k},j})\Big]. \quad (20)$$

Finally, after the Bogoliubov transformation of Eqs. (11) and (12) we get

$$\begin{aligned} V_{LSW} = & \sqrt{S}\sum_j \sum_{\boldsymbol{k}} g(\omega_j)\left(\tfrac{d-\xi_{\boldsymbol{k}}}{d+\xi_{\boldsymbol{k}}}\right)^{1/4} \\ & \times\Big[(\alpha_{\boldsymbol{k}}+\beta^\dagger_{\boldsymbol{k}})(A_{-\boldsymbol{k},j}+A^\dagger_{\boldsymbol{k},j}) \\ & +(\alpha^\dagger_{\boldsymbol{k}}+\beta_{\boldsymbol{k}})(A_{\boldsymbol{k},j}+A^\dagger_{-\boldsymbol{k},j})\Big]. \end{aligned} \tag{21}$$

IV. MASTER EQUATION FOR A THERMAL ENVIRONMENT

The dynamics of system and environment is given by the von Neumann equation

$$\frac{d\rho}{dt} = -\frac{\mathrm{i}}{\hbar}[H,\rho], \tag{22}$$

where

$$H = H_{LSW} + H_E + V_{LSW}. \tag{23}$$

We aim at writing a dynamical equation for the state of the system $\rho_S = \mathrm{Tr}_E(\rho)$, where the trace is taken over the environment degrees of freedom. This task is generally quite complicated. However, we are particularly interested in describing how the system evolves to the Gibbs state because the lack of insulation; and such a case is expected to happen for a large environment in thermal equilibrium (a "bath") with a small coupling constant. Under these conditions an equation, called master equation, can be found by resorting to perturbation theory [19].

The initial state of the environment is then written as

$$\begin{aligned} \rho_E = Z^{-1}\mathrm{e}^{-\beta H_E} &= Z^{-1}\mathrm{e}^{-\beta\sum_j\sum_{\boldsymbol{r}}\omega_j A^\dagger_{\boldsymbol{r},j}A_{\boldsymbol{r},j}} \\ &= Z^{-1}\mathrm{e}^{-\beta\sum_j\sum_{\boldsymbol{k}}\omega_j A^\dagger_{\boldsymbol{k},j}A_{\boldsymbol{k},j}}, \end{aligned} \tag{24}$$

where $Z=\mathrm{Tr}\left(\mathrm{e}^{-\beta H_E}\right)$ is the partition function with $\beta = 1/k_{\mathrm{B}}T$. From now on we shall use natural units $\hbar = k_{\mathrm{B}} = 1$.

Because of the Riemann-Lebesgue lemma [4], for small coupling $g(\omega_j)$ we can safely neglect the counter-rotating terms in (21),

$$\begin{aligned} V_{LSW} = & \sqrt{S}\sum_j\sum_{\boldsymbol{k}} g(\omega_j)\left(\tfrac{d-\xi_{\boldsymbol{k}}}{d+\xi_{\boldsymbol{k}}}\right)^{1/4}\Big[\alpha_{\boldsymbol{k}}A^\dagger_{\boldsymbol{k},j} \\ & +\beta^\dagger_{\boldsymbol{k}}A_{-\boldsymbol{k},j}+\alpha^\dagger_{\boldsymbol{k}}A_{\boldsymbol{k},j}+\beta_{\boldsymbol{k}}A^\dagger_{-\boldsymbol{k},j}\Big]. \end{aligned} \tag{25}$$

Now the problem becomes equivalent to two collections of uncoupled harmonic oscillators given by their operators $\alpha_{\boldsymbol{k}}$ and $\beta_{\boldsymbol{k}}$, which are coupled to set of independent environments characterized by $\boldsymbol{k}$. The standard tools to obtain a master equation for a weak interaction with the environment can be found in references [4–7]. If we apply those techniques to this system we arrive at

$$\begin{aligned} \frac{d\rho}{dt} = \mathcal{L}(\rho) = & -\mathrm{i}[H_{LSW},\rho] \\ & + \sum_{\boldsymbol{k}}\gamma_{\boldsymbol{k}}(\bar{n}_{\boldsymbol{k}}+1)\left(\alpha_{\boldsymbol{k}}\rho\alpha^\dagger_{\boldsymbol{k}}-\frac{1}{2}\{\alpha^\dagger_{\boldsymbol{k}}\alpha_{\boldsymbol{k}},\rho\}+\beta_{\boldsymbol{k}}\rho\beta^\dagger_{\boldsymbol{k}}-\frac{1}{2}\{\beta^\dagger_{\boldsymbol{k}}\beta_{\boldsymbol{k}},\rho\}\right) \\ & + \gamma_{\boldsymbol{k}}\bar{n}_{\boldsymbol{k}}\left(\alpha^\dagger_{\boldsymbol{k}}\rho\alpha_{\boldsymbol{k}}-\frac{1}{2}\{\alpha_{\boldsymbol{k}}\alpha^\dagger_{\boldsymbol{k}},\rho\}+\beta^\dagger_{\boldsymbol{k}}\rho\beta_{\boldsymbol{k}}-\frac{1}{2}\{\beta_{\boldsymbol{k}}\beta^\dagger_{\boldsymbol{k}},\rho\}\right) \\ & + \gamma_{\boldsymbol{k}}(\bar{n}_{\boldsymbol{k}}+1)\left(\alpha_{\boldsymbol{k}}\rho\beta^\dagger_{-\boldsymbol{k}}-\frac{1}{2}\{\beta^\dagger_{-\boldsymbol{k}}\alpha_{\boldsymbol{k}},\rho\}+\beta_{-\boldsymbol{k}}\rho\alpha^\dagger_{\boldsymbol{k}}-\frac{1}{2}\{\alpha^\dagger_{\boldsymbol{k}}\beta_{-\boldsymbol{k}},\rho\}\right) \\ & + \gamma_{\boldsymbol{k}}\bar{n}_{\boldsymbol{k}}\left(\beta^\dagger_{-\boldsymbol{k}}\rho\alpha_{\boldsymbol{k}}-\frac{1}{2}\{\alpha_{\boldsymbol{k}}\beta^\dagger_{-\boldsymbol{k}},\rho\}+\alpha^\dagger_{\boldsymbol{k}}\rho\beta_{-\boldsymbol{k}}-\frac{1}{2}\{\beta_{-\boldsymbol{k}}\alpha^\dagger_{\boldsymbol{k}},\rho\}\right). \end{aligned} \tag{26}$$

Here

$$\gamma_{\boldsymbol{k}} := 2\pi S\sqrt{\frac{d-\xi_{\boldsymbol{k}}}{d+\xi_{\boldsymbol{k}}}}\mathcal{J}(\omega(\boldsymbol{k})), \tag{27}$$

where $\mathcal{J}(\omega)=\sum_j g^2(\omega)\delta(\omega-\omega_j)$ is the so-called "spectral density" of the bath. This one, for solid state environments, is usually parameterized in the continuous limit [5, 18] as

$$\mathcal{J}(\omega) = \alpha\omega^s\omega_c^{s-1}\mathrm{e}^{-\omega/\omega_c}, \tag{28}$$

where α accounts for the strength of the coupling and ω_c is the cut-off frequency of the bath. Typically three cases are distinguished, $s>1$ (super-ohmic), $s=1$ (ohmic) and $s<1$ (sub-ohmic). The other quantity $\bar{n}$ is the mean number of phonons in the bath with frequency $\omega(\boldsymbol{k})$,

$$\bar{n}_{\boldsymbol{k}} := [\exp(\omega(\boldsymbol{k})/T)-1]^{-1}. \tag{29}$$

Note the presence of the crossing terms "$\alpha(\cdot)\beta^\dagger$" in the master equation. They are absent in the analogous treatment of a ferromagnetic system and they will be induce a different rate for the decay of the magnetic order, for

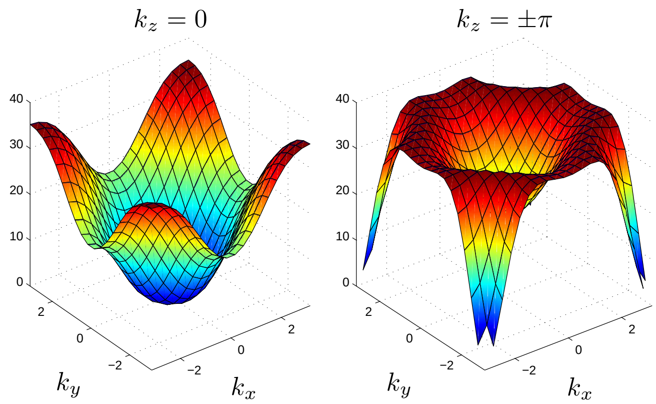

FIG. 2: Magnon decay rate (27) in the first Brillouin zone. On the left it is depicted the surface for $k_z = 0$ and $k_z = \pm\pi$ is on the right.

instance.

A. Approach to the Equilibrium

By construction [19], the Gibbs state $\rho_{\rm th} = Z^{-1}{\rm e}^{-H_{LSW}/T}$, at the same temperature T as the bath, is the steady state of equation (26), i.e. $\mathcal{L}(\rho_{\rm th}) = 0$. This is straightforwardly verified by taking into account that

$$
\begin{aligned}
{\rm e}^{-H_{LSW}/T}\alpha_{\boldsymbol{k}} &= {\rm e}^{\omega(\boldsymbol{k})/T}\alpha_{\boldsymbol{k}}{\rm e}^{-H_{LSW}/T}, \quad (30)\\
{\rm e}^{-H_{LSW}/T}\beta_{\boldsymbol{k}} &= {\rm e}^{\omega(\boldsymbol{k})/T}\beta_{\boldsymbol{k}}{\rm e}^{-H_{LSW}/T}. \quad (31)
\end{aligned}
$$

Moreover any initial state of the system becomes closer and closer to this Gibbs state during time evolution.

We have thus constructed a dynamical equation to describe the thermal relaxation process of a quantum antiferromagnet. Remember that for the spin wave theory to make sense the number of magnons has to be small (6), so for large bath temperatures this treatment is not valid in the long time limit where the state approaches to the Gibbs' (which contains a large number of magnons for large T). However the predictions of equation (26) should also agree reasonably well with the exact ones at short times.

B. Magnon Decay Rates

A remarkable property of this system is that every exponent is not allowed in the spectral density (28) in order to obtain finite results for many-body observables. This is because quantities such as magnon decay rates (27) and the thermal number of phonons become infinite for certain values of $\boldsymbol{k}$, so for those values the spectral density has to approach zero fast enough. Particularly, it requires a super-Ohmic spectral density. It is worth to remind here that these kind of problems may also arise in simpler systems, for instance in a single spin when subject to a pure dephasing environment (see [4]). The concrete values of the rest of parameters of $\mathcal{J}(\omega)$ is not very relevant for our proposes as we always assume to be in a sufficiently weak interaction regime [20], we shall take

$$
s = 3, \quad \alpha = J/10, \quad \omega_c = \max_{\boldsymbol{k}} \omega(\boldsymbol{k}) = 2JSd. \quad (32)
$$

In figure 2 we have represented two sheets of the magnon decay rate (27) in the first Brillouin zone. On one hand, we note that the magnon decay rate vanishes on the origin and on the eight corners of the Brillouin zone $\boldsymbol{k} = (\pm\pi, \pm\pi, \pm\pi)$. On the other hand it reaches the maximum value on the points of a sphere of radious $r \simeq 0.947$ centered just this eight minimum points $\boldsymbol{k} = (\pm\pi, \pm\pi, \pm\pi)$. Between both cases there is a transition which we have tried to illustrate by taken the values $k_z = 0, \pm\pi$ in the figure (given the symmetry of the decay rate, we can use $k_{x,y}$ instead of k_z leading to the same figures).

From (26) it is possible to compute the evolution of any combination of $\alpha_{\boldsymbol{k}}$ and $\beta_{\boldsymbol{k}}$ in the Heiserberg picture. We give the result for the evolution of the first and second moments in Appendix A. Those expressions allows us to compute the evolution of any spin operator in the quantum antiferromagnet and relevant observables constructed out of them.

V. DYNAMICS OF RELEVANT OBSERVABLES

In this section we study the time-evolution of some properties which have special interest in the description a quantum antiferromagnet. For concreteness, we have selected two of them, the staggered magnetization and the spin correlation functions.

A. Staggered magnetization

Due to the isotropy of Hamiltonian (1), one may expect the ground state to be also symmetric under rotations. However, as we have already mentioned, the ground state turns out to be close to the Néel state, which has clearly a privileged orientation. This is an example of spontaneous symmetry breaking [14] . The figure of merit to compute this order in a quantum antiferromagnet is the expectation value of the staggered magnetization operator

$$
\hat{m}_z^{\rm st} = \frac{1}{N}\sum_{\boldsymbol{r}} (-1)^{\|\boldsymbol{r}\|} S_{\boldsymbol{r}}^z, \quad (33)
$$

which in the thermodynamic limit reads

$$
m^{\rm st} = \lim_{N\to\infty} \langle \hat{m}_z^\dagger \rangle = \lim_{N\to\infty} \frac{1}{N}\sum_{\boldsymbol{r}} (-1)^{\|\boldsymbol{r}\|} \langle S_{\boldsymbol{r}}^z \rangle. \quad (34)
$$

By using the equations (2) and (3), we may write this operator as

$$\hat{m}_z^{\rm st} = \frac{1}{N}\sum_{\boldsymbol{r}}(S-n_{\boldsymbol{r}}) = S-\frac{1}{N}\sum_{\boldsymbol{r}}\hat{n}_{\boldsymbol{r}} = S-\frac{1}{N}\sum_{\boldsymbol{k}}\hat{n}_{\boldsymbol{k}}, \quad (35)$$

with $\hat{n}_{\boldsymbol{k}} = \hat{n}_{\boldsymbol{k}}^{(a)} + \hat{n}_{\boldsymbol{k}}^{(b)}$. Note that $\boldsymbol{k} = 2\pi\boldsymbol{m}/(N/2)$ where $\boldsymbol{m}$ varies two by two instead of one by one. So in the thermodynamic limit

$$\lim_{N\to\infty}\frac{1}{N}\sum_{\boldsymbol{k}} = \frac{1}{2(2\pi)^3}\int_{\rm B.Z.} d\boldsymbol{k}. \quad (36)$$

Here B.Z. denotes the first Brillouin zone, and the extra factor 1/2 appears because the double spacing between consecutive $\boldsymbol{k}$ on the left hand side. Thus, the staggered magnetization becomes

$$m^{\rm st} = S - \frac{1}{16\pi^3}\int_{\rm B.Z.} d\boldsymbol{k}\langle\hat{n}_{\boldsymbol{k}}\rangle. \quad (37)$$

When the system is interacting with a thermal bath, the staggered magnetization approaches in time to its thermal value. This is exactly zero for any $T \neq 0$ due to de Mermin-Wagner theorem [21] in 1D and 2D, however that is not the case in 3D. Additionally, note that the interaction Hamiltonian (16) is also isotropic so it is not trivial to find also magnetic order when the quantum antiferromagnetic is not isolated.

From the master equation (26) we are able to visualize how staggered magnetization varies as a function of time. For this aim we just need to find the evolution of the observables $\hat{n}_{\boldsymbol{k}}$. In terms of the operators $\alpha_{\boldsymbol{k}}$ and $\beta_{\boldsymbol{k}}$, we have

$$\begin{aligned}\hat{n}_{\boldsymbol{k}}^{(a)} &= \cosh^2(\theta_{\boldsymbol{k}})\alpha_{\boldsymbol{k}}^\dagger\alpha_{\boldsymbol{k}} \\ &- \sinh(\theta_{\boldsymbol{k}})\cosh(\theta_{\boldsymbol{k}})(\alpha_{\boldsymbol{k}}^\dagger\beta_{\boldsymbol{k}}^\dagger \\ &+ \alpha_{\boldsymbol{k}}\beta_{\boldsymbol{k}}) + \sinh^2(\theta_{\boldsymbol{k}})(\beta_{\boldsymbol{k}}^\dagger\beta_{\boldsymbol{k}}+1), \quad (38)\\ \hat{n}_{\boldsymbol{k}}^{(b)} &= \sinh^2(\theta_{\boldsymbol{k}})(\alpha_{\boldsymbol{k}}^\dagger\alpha_{\boldsymbol{k}}+1) \\ &- \sinh(\theta_{\boldsymbol{k}})\cosh(\theta_{\boldsymbol{k}})(\alpha_{\boldsymbol{k}}^\dagger\beta_{\boldsymbol{k}}^\dagger + \alpha_{\boldsymbol{k}}\beta_{\boldsymbol{k}}) \\ &+ \cosh^2(\theta_{\boldsymbol{k}})\beta_{\boldsymbol{k}}^\dagger\beta_{\boldsymbol{k}}. \quad (39)\end{aligned}$$

Particularly, if we start from the ground state, $\langle\alpha_{\boldsymbol{k}}^\dagger\alpha_{\boldsymbol{k}}(0)\rangle = \langle\beta_{\boldsymbol{k}}^\dagger\beta_{\boldsymbol{k}}(0)\rangle = \langle\alpha_{\boldsymbol{k}}\beta_{\boldsymbol{k}}(0)\rangle = 0$, we find

$$\langle\hat{n}_{\boldsymbol{k}}^{(a)}(t)\rangle = \langle\hat{n}_{\boldsymbol{k}}^{(b)}(t)\rangle = \cosh(2\theta_{\boldsymbol{k}})\bar{n}_{\boldsymbol{k}}\left[1-{\rm e}^{-\gamma_{\boldsymbol{k}}t}\cos(\gamma_{\boldsymbol{k}}t)\right] + \sinh^2(\theta_{\boldsymbol{k}}).$$

Introducing these values in (37) and using equation (13):

$$m^{\rm st} = m_0^{\rm st} - \frac{d}{8\pi^3}\int_{\rm B.Z.} d\boldsymbol{k}\left[\frac{\bar{n}_{\boldsymbol{k}}}{\sqrt{d^2-\xi_{\boldsymbol{k}}^2}}\right]\left[1-{\rm e}^{-\gamma_{\boldsymbol{k}}t}\cos(\gamma_{\boldsymbol{k}}t)\right], \quad (40)$$

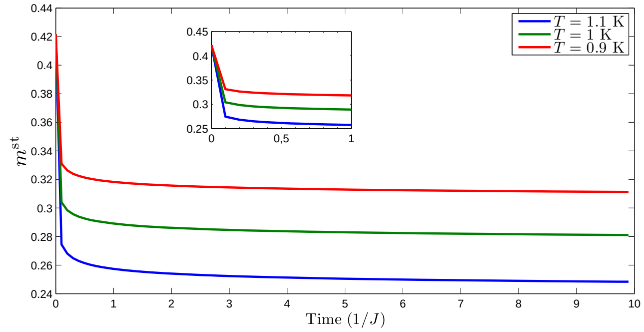

FIG. 3: Decay of the staggered magnetization showing the approach to the Gibbs state values $m_\beta^{\rm st}$. The red line corresponds to $T = 0.9$ K with $m_\beta^{\rm st} \simeq 0.302$, for the green line $T = 1$ K and $m_\beta^{\rm st} \simeq 0.271$, and for the blue line $T = 1.1$ K and $m_\beta^{\rm st} \simeq 0.237$. The inset shows more in detail the evolution at short times.

where

$$m_0^{\rm st} = S - \frac{1}{16\pi^3}\int_{\rm B.Z.} d\boldsymbol{k}\left(\frac{d}{\sqrt{d^2-\xi_{\boldsymbol{k}}^2}}-1\right) \quad (41)$$

is the expectation value of the staggered magnetization in the ground state. In 3D, for a square lattice and $S = 1/2$ this value is $m_0^{\rm st} \simeq 0.422$.

In figure 3, the evolution of the staggered magnetization is shown for different values of the bath temperature. It is noteworthy to mention the non-exponential decay of $m^{\rm st}$. This is due to its dependence on t through the integral of (40), which renders combinations of different exponentials. Remarkably, there is a short period where the order is lost very fast (between $t = 0$ and $t \sim 0.1/J$, see inset figure). After that, the system continues evolving slower to the Gibbs state. This suggests that if we want to visualize variations of $m^{\rm st}$ due to the environment, the best chance is to look for them in systems with not very small J.

B. Two-point correlation functions

It is also worthwhile to study the second moments of angular momentum operators. For the sake of illustration, we focus in this section in the transversal two-point spatial correlation function, which is

$$S_\perp(\boldsymbol{r}_1,\boldsymbol{r}_2,t) = {\rm Tr}[S_{\boldsymbol{r}_1}^x S_{\boldsymbol{r}_2}^x\rho(t)]. \quad (42)$$

Without lost of generality we take $\boldsymbol{r}_1 \in A$. Then for $\boldsymbol{r}_2 \in A$

$$S_\perp(\boldsymbol{r}_1,\boldsymbol{r}_2,t) = \frac{S}{2}{\rm Tr}[(a_{\boldsymbol{r}_1}+a_{\boldsymbol{r}_1}^\dagger)(a_{\boldsymbol{r}_2}+a_{\boldsymbol{r}_2}^\dagger)\rho(t)], \quad (43)$$

and

$$S_\perp(\boldsymbol{r}_1,\boldsymbol{r}_2,t) = \frac{S}{2}{\rm Tr}[(a_{\boldsymbol{r}_1}+a_{\boldsymbol{r}_1}^\dagger)(b_{\boldsymbol{r}_2}+b_{\boldsymbol{r}_2}^\dagger)\rho(t)], \quad (44)$$

for $\boldsymbol{r}_2 \in B$.

Details of the computation are found in Appendix B, finally in the thermodynamic limit we obtain

$$S_\perp(\boldsymbol{r}_1,\boldsymbol{r}_2,t) = \frac{S}{2(2\pi)^3}\int_{\text{B.Z.}} d\boldsymbol{k}\cos[\boldsymbol{k}\cdot(\boldsymbol{r}_1-\boldsymbol{r}_2)]\left(\frac{\Theta(\boldsymbol{r}_2)\{1+2\bar{n}_{\boldsymbol{k}}[1-\mathrm{e}^{-\gamma_{\boldsymbol{k}}t}\cos(\gamma_{\boldsymbol{k}}t)]\}+\tilde{\Theta}(\boldsymbol{r}_2)2\bar{n}_{\boldsymbol{k}}\,\mathrm{e}^{-\gamma_{\boldsymbol{k}}t}\sin(\gamma_{\boldsymbol{k}}t)}{\sqrt{d^2-\xi_{\boldsymbol{k}}^2}}\right), \tag{45}$$

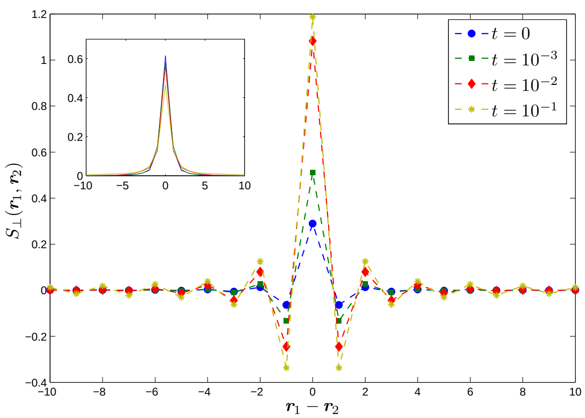

FIG. 4: Evolution of $S_\perp(\boldsymbol{r}_1,\boldsymbol{r}_2,t)$ for $T=5$ K in the thermodynamic limit for different time instants (in units of J^{-1}). Note the oscillating behaviour typical of antiferromagnetics systems. The inset figure illustrates the similarity between the cases for $|S_\perp(\boldsymbol{r}_1,\boldsymbol{r}_2,t)|$ after normalization.

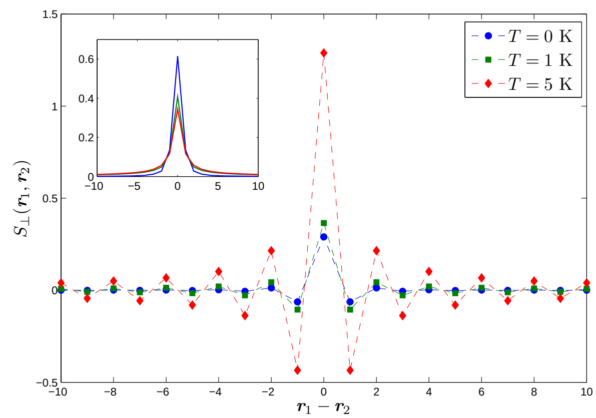

FIG. 5: Thermal values of $S_\perp(\boldsymbol{r}_1,\boldsymbol{r}_2)$. In the inset is represented again its normalized absolute value.

where

$$\Theta_{\boldsymbol{k}}(\boldsymbol{r}) = \begin{cases} d, & \text{if } \boldsymbol{r}\in A,\\ -\xi_{\boldsymbol{k}}, & \text{if } \boldsymbol{r}\in B,\end{cases} \tag{46}$$

and

$$\tilde{\Theta}_{\boldsymbol{k}}(\boldsymbol{r}) = \begin{cases} -\xi_{\boldsymbol{k}}, & \text{if } \boldsymbol{r}\in A,\\ d, & \text{if } \boldsymbol{r}\in B.\end{cases} \tag{47}$$

We have plotted this correlation for some time instants in figure 4. In addition, figure 5 shows different cases when the Gibbs states has been reached.

C. Response function

Other interesting quantities in this system are the response functions. They are the Fourier transform of two-time correlation functions of spin operators, and for instance, they directly appear in cross sections of inelastic neutron scattering, which are experimentally accessible. For an antiferromagnet with staggered magnetization in the z direction the inelastic scattering is related to the correlation $\langle S^x_{-\boldsymbol{k}}(t+\tau)S^x_{\boldsymbol{k}}(t)\rangle$, where

$$S^x_{\boldsymbol{k}} = \frac{1}{\sqrt{N}}\sum_{\boldsymbol{r}}\mathrm{e}^{\mathrm{i}\boldsymbol{k}\cdot\boldsymbol{r}}S^x_{\boldsymbol{r}}. \tag{48}$$

One has to be specially careful when computing multitime-correlation functions for non-unitary evolutions. This is because the evolution of the product of two operators, say a and b, does not equal to the product of the individual evolutions of a and b when the dynamics is not unitary, i.e. $(ab)(t)\neq a(t)b(t)$. However we can circumvent this problem by writing the correlation function on the extended space where the evolution is indeed unitary

$$\begin{aligned}\langle 0|S^x_{-\boldsymbol{k}}(t+\tau)S^x_{\boldsymbol{k}}(t)|0\rangle &= \mathrm{Tr}\langle[S^x_{-\boldsymbol{k}}(t+\tau)S^x_{\boldsymbol{k}}(t)|0\rangle\langle 0|\otimes\rho_E]\\ &= \mathrm{Tr}\left[\mathrm{e}^{\mathrm{i}H(t+\tau)}S^x_{-\boldsymbol{k}}\mathrm{e}^{-\mathrm{i}H\tau}S^x_{\boldsymbol{k}}\mathrm{e}^{-\mathrm{i}Ht}|0\rangle\langle 0|\otimes\rho_E\right].\end{aligned}$$

Here the trace operation is taken over both system and environment degrees of freedom, and $H = H_{LSW}+H_E+V_{LSW}$ is the whole Hamiltonian of system and environment. Then it is possible to obtain that (see detailed discussion in [7])

$$\langle 0|S^x_{-\boldsymbol{k}}(t+\tau)S^x_{\boldsymbol{k}}(t)|0\rangle = \langle 0|\left[S^x_{-\boldsymbol{k}}(\tau)S^x_{\boldsymbol{k}}\right](t)|0\rangle. \tag{49}$$

That is, it is needed to obtain first the Heisenberg evolution with respect to the parameter τ of the operator $S^x_{-\boldsymbol{k}}$ and after that, the Heisenberg evolution with respect to the parameter t of the product $S^x_{-\boldsymbol{k}}(\tau)S^x_{\boldsymbol{k}}$.

For linear spin-wave theory we have

$$S^x_{\boldsymbol{r}} = \frac{S^+_{\boldsymbol{r}} + S^-_{\boldsymbol{r}}}{2} = \sqrt{\frac{S}{2}} \begin{cases} a_{\boldsymbol{r}} + a^\dagger_{\boldsymbol{r}}, & \text{if } \boldsymbol{r} \in A, \\ b_{\boldsymbol{r}} + b^\dagger_{\boldsymbol{r}}, & \text{if } \boldsymbol{r} \in B, \end{cases} \tag{50}$$

thus, according to (7) and (48),

$$S^x_{\boldsymbol{k}} = \frac{\sqrt{S}}{2}(a_{\boldsymbol{k}} + a^\dagger_{-\boldsymbol{k}} + b_{-\boldsymbol{k}} + b^\dagger_{\boldsymbol{k}}). \tag{51}$$

If we perform the Bogoliubov transformation (11) and (12), the Eqs. (A1) and (A2) lead to

$$\begin{aligned} S^x_{-\boldsymbol{k}}(\tau) &= \frac{\sqrt{S}}{2}\mathrm{e}^{-\gamma_{\boldsymbol{k}}\tau/2}[\cosh(\theta_{\boldsymbol{k}}) - \sinh(\theta_{\boldsymbol{k}})]\Big(\mathrm{e}^{-\mathrm{i}\omega(\boldsymbol{k})\tau}\left\{[\cos(\gamma_{\boldsymbol{k}}\tau/2) + \sin(\gamma_{\boldsymbol{k}}\tau/2)]\alpha_{-\boldsymbol{k}} + [\cos(\gamma_{\boldsymbol{k}}\tau/2) - \sin(\gamma_{\boldsymbol{k}}\tau/2)]\beta_{\boldsymbol{k}}\right\} \\ &+ \mathrm{e}^{\mathrm{i}\omega(\boldsymbol{k})\tau}\left\{[\cos(\gamma_{\boldsymbol{k}}\tau/2) + \sin(\gamma_{\boldsymbol{k}}\tau/2)]\alpha^\dagger_{\boldsymbol{k}} + [\cos(\gamma_{\boldsymbol{k}}\tau/2) - \sin(\gamma_{\boldsymbol{k}}\tau/2)]\beta^\dagger_{-\boldsymbol{k}}\right\}\Big), \end{aligned} \tag{52}$$

where we have used the fact that $\theta_{-\boldsymbol{k}} = \theta_{\boldsymbol{k}}$ and $\omega(-\boldsymbol{k}) = \omega(\boldsymbol{k})$. Since by assumption $\gamma_{\boldsymbol{k}}$ is small, for small τ we can neglect it in comparison to the complex exponential $\mathrm{e}^{\pm\mathrm{i}\omega(\boldsymbol{k})\tau}$,

$$S^x_{-\boldsymbol{k}}(\tau) \simeq \frac{\sqrt{S}}{2}[\cosh(\theta_{\boldsymbol{k}}) - \sinh(\theta_{\boldsymbol{k}})]\left[\mathrm{e}^{-\mathrm{i}\omega(\boldsymbol{k})\tau}(\alpha_{-\boldsymbol{k}} + \beta_{\boldsymbol{k}}) + \mathrm{e}^{\mathrm{i}\omega(\boldsymbol{k})\tau}(\alpha^\dagger_{\boldsymbol{k}} + \beta^\dagger_{-\boldsymbol{k}})\right]. \tag{53}$$

Finally, by using (A4) and (A5), we compute the evolution of $S^x_{-\boldsymbol{k}}(\tau)S^x_{\boldsymbol{k}}$ with respect to t, and after simplifying vanishing terms the correlation function reads

$$\begin{aligned} \langle S^x_{-\boldsymbol{k}}(t+\tau)S^x_{\boldsymbol{k}}(t)\rangle &= \frac{S}{4}[\cosh(2\theta_{\boldsymbol{k}}) - \sinh(2\theta_{\boldsymbol{k}})]\Big\{\mathrm{e}^{-\mathrm{i}\omega(\boldsymbol{k})\tau}[\langle\alpha_{-\boldsymbol{k}}\alpha^\dagger_{-\boldsymbol{k}}(t)\rangle + \langle\beta_{\boldsymbol{k}}\beta^\dagger_{\boldsymbol{k}}(t)\rangle + \langle\alpha^\dagger_{-\boldsymbol{k}}\beta_{\boldsymbol{k}}(t)\rangle + \langle\alpha_{-\boldsymbol{k}}\beta^\dagger_{\boldsymbol{k}}(t)\rangle] \\ &+ \mathrm{e}^{\mathrm{i}\omega(\boldsymbol{k})\tau}[\langle\alpha^\dagger_{\boldsymbol{k}}\alpha_{\boldsymbol{k}}(t)\rangle + \langle\beta^\dagger_{-\boldsymbol{k}}\beta_{-\boldsymbol{k}}(t)\rangle + \langle\alpha^\dagger_{\boldsymbol{k}}\beta_{-\boldsymbol{k}}(t)\rangle + \langle\alpha_{\boldsymbol{k}}\beta^\dagger_{-\boldsymbol{k}}(t)\rangle]\Big\} \\ &= \frac{S(d-\xi_{\boldsymbol{k}})}{2\sqrt{d^2-\xi^2_{\boldsymbol{k}}}}\Big(\mathrm{e}^{-\mathrm{i}\omega(\boldsymbol{k})\tau}\left\{\bar{n}_{\boldsymbol{k}}\left[1 - \mathrm{e}^{-\gamma_{\boldsymbol{k}}t}\cos(\gamma_{\boldsymbol{k}}t) + 2\sin(\gamma_{\boldsymbol{k}}t)\right] + 1\right\} \\ &+ \mathrm{e}^{\mathrm{i}\omega(\boldsymbol{k})\tau}\bar{n}_{\boldsymbol{k}}\left[1 - \mathrm{e}^{-\gamma_{\boldsymbol{k}}t}\cos(\gamma_{\boldsymbol{k}}t) + 2\sin(\gamma_{\boldsymbol{k}}t)\right]\Big). \end{aligned} \tag{54}$$

The Fourier transform with respect to τ leads to the response function:

$$S_\perp(\boldsymbol{k},t,\omega) = S^-_{LSQ}(\boldsymbol{k},t)\delta[\omega-\omega(\boldsymbol{k})] + S^+_{LSQ}(\boldsymbol{k},t)\delta[\omega+\omega(\boldsymbol{k})], \tag{55}$$

with

$$\begin{aligned} S^-_{LSQ}(\boldsymbol{k},t) &= \frac{S(d-\xi_{\boldsymbol{k}})}{2\sqrt{d^2-\xi^2_{\boldsymbol{k}}}}\left\{\bar{n}_{\boldsymbol{k}}\left[1 - \mathrm{e}^{-\gamma_{\boldsymbol{k}}t}\cos(\gamma_{\boldsymbol{k}}t)\right.\right. \\ &+ \left.\left. 2\sin(\gamma_{\boldsymbol{k}}t)\right] + 1\right\}, \end{aligned} \tag{56}$$

$$\begin{aligned} S^+_{LSQ}(\boldsymbol{k},t) &= \frac{S(d-\xi_{\boldsymbol{k}})}{2\sqrt{d^2-\xi^2_{\boldsymbol{k}}}}\bar{n}_{\boldsymbol{k}}\left[1 - \mathrm{e}^{-\gamma_{\boldsymbol{k}}t}\cos(\gamma_{\boldsymbol{k}}t)\right. \\ &+ \left. 2\sin(\gamma_{\boldsymbol{k}}t)\right]. \end{aligned} \tag{57}$$

Therefore, at $t = 0$ (or $T = 0$) only the form factor $S^-_{LSQ}(\boldsymbol{k},t)$ remains. On the other hand we conclude that as temperature increases, $S^\pm_{LSQ}(\boldsymbol{k},t)$ also increases, and they have the same geometry in momentum space as the magnon decay rates $\gamma_{\boldsymbol{k}}$. However the behaviour with time is not monotonic, $S^\pm_{LSQ}(\boldsymbol{k},t)$ starts increasing with time until it reaches its maximum value at $t_{\max} = \arccos(1/\sqrt{10})/\gamma_{\boldsymbol{k}}$, after this point it decreases monotonically towards the thermal value.

VI. CONCLUSIONS

In this work we have analyzed the behaviour of a quantum antiferromagnet in contact with a boson thermal bath. Based on spin wave theory, we have applied the weak coupling procedure (Davies' theory) to obtain a master equation for the dynamics. We belief this is a basic and fundamental problem which has remained quite unexplored so far. It is at the crossroads of strongly correlated systems and the physics of quantum open systems that is so much rooted in quantum information theory.

From the open systems point of view, spin wave theory provides us with a nice framework to apply the well-known techniques developed for quantum optics or quantum chemistry settings to quantum many-body problems. Interestingly, some features which are typically encountered in small systems under weak coupling limit, e.g. the exponential decay of observables, may be lost when computing the observables which are relevant for the many-body systems. We have exemplified this point by studying the staggered magnetization, which for moderate temperatures, and despite of the the isotropic cou-

pling to the bath does not vanish. In fact, it does not shows an exponential decay either.

Furthermore, we have illustrated the versatility of our master equation approach to the dynamics of thermal effects in quantum antiferromagnets by computing two-point correlation and response functions, also known as form factors. The geometry in momentum space of these response functions $S_{LSQ}(\boldsymbol{k},t)$ are closely related to that of the decay rate function in the first Brillouin zone. These form factors, in turn, are directly related to differential cross-sections in experiments of inelastic neutron scattering which we believe that may shed light to the current knowledge of a quantum antiferromagnet under non-isolated situations.

Acknowledgments

We thank the Spanish MICINN grant FIS2009-10061, CAM research consortium QUITEMAD S2009-ESP-1594, European Commission PICC: FP7 2007-2013, Grant No. 249958, UCM-BS grant GICC-910758.

Appendix A: Time-evolution of the first and second moments

The generator $\mathcal{L}^\sharp$ in Heisenberg picture is obtained by the equality $\mathrm{Tr}[X\mathcal{L}(\rho)] = \mathrm{Tr}[\rho\mathcal{L}^\sharp(X)]$, for any operator X. By solving the dynamical equations, we obtain

$$\begin{aligned}
\alpha_{\boldsymbol{k}}(t) &= \mathrm{e}^{[-\mathrm{i}\omega(\boldsymbol{k})-\gamma_{\boldsymbol{k}}/2]t}[\cos(\gamma_{\boldsymbol{k}}t/2)\alpha_{\boldsymbol{k}}(0) - \sin(\gamma_{\boldsymbol{k}}t/2)\beta_{-\boldsymbol{k}}(0)\}, && \text{(A1)}\\
\beta_{\boldsymbol{k}}(t) &= \mathrm{e}^{[-\mathrm{i}\omega(\boldsymbol{k})-\gamma_{\boldsymbol{k}}/2]t}[\sin(\gamma_{\boldsymbol{k}}t/2)\alpha_{-\boldsymbol{k}}(0) + \cos(\gamma_{\boldsymbol{k}}t/2)\beta_{\boldsymbol{k}}(0)], && \text{(A2)}\\
\alpha_{\boldsymbol{k}}\beta^\dagger_{-\boldsymbol{k}}(t) &= \tfrac{1}{2}\mathrm{e}^{-\gamma_{\boldsymbol{k}}t}\Big\{[\cos(\gamma_{\boldsymbol{k}}t)+1]\alpha_{\boldsymbol{k}}\beta^\dagger_{-\boldsymbol{k}}(0) + [\cos(\gamma_{\boldsymbol{k}}t)-1]\alpha^\dagger_{\boldsymbol{k}}\beta_{-\boldsymbol{k}}(0)\\
&- \sin(\gamma_{\boldsymbol{k}}t)[\alpha^\dagger_{\boldsymbol{k}}\alpha_{\boldsymbol{k}}(0) + \beta^\dagger_{-\boldsymbol{k}}\beta_{-\boldsymbol{k}}(0) - 2\bar{n}_{\boldsymbol{k}}]\Big\}, && \text{(A3)}\\
\alpha^\dagger_{\boldsymbol{k}}\alpha_{\boldsymbol{k}}(t) &= \tfrac{1}{2}\mathrm{e}^{-\gamma_{\boldsymbol{k}}t}\Big\{[\cos(\gamma_{\boldsymbol{k}}t)+1]\alpha^\dagger_{\boldsymbol{k}}\alpha_{\boldsymbol{k}}(0) + [\cos(\gamma_{\boldsymbol{k}}t)-1]\beta^\dagger_{-\boldsymbol{k}}\beta_{-\boldsymbol{k}}(0)\\
&+ \sin(\gamma_{\boldsymbol{k}}t)[\alpha_{\boldsymbol{k}}\beta^\dagger_{-\boldsymbol{k}}(0) + \alpha^\dagger_{\boldsymbol{k}}\beta_{-\boldsymbol{k}}(0)]\Big\} + \bar{n}_{\boldsymbol{k}}[1-\mathrm{e}^{-\gamma_{\boldsymbol{k}}t}\cos(\gamma_{\boldsymbol{k}}t)], && \text{(A4)}\\
\beta^\dagger_{\boldsymbol{k}}\beta_{\boldsymbol{k}}(t) &= \tfrac{1}{2}\mathrm{e}^{-\gamma_{\boldsymbol{k}}t}\Big\{[\cos(\gamma_{\boldsymbol{k}}t)-1]\alpha^\dagger_{-\boldsymbol{k}}\alpha_{-\boldsymbol{k}}(0) + [\cos(\gamma_{\boldsymbol{k}}t)+1]\beta^\dagger_{\boldsymbol{k}}\beta_{\boldsymbol{k}}(0)\\
&+ \sin(\gamma_{\boldsymbol{k}}t)[\alpha_{-\boldsymbol{k}}\beta^\dagger_{\boldsymbol{k}}(0) + \alpha^\dagger_{-\boldsymbol{k}}\beta_{\boldsymbol{k}}(0)]\Big\} + \bar{n}_{\boldsymbol{k}}[1-\mathrm{e}^{-\gamma_{\boldsymbol{k}}t}\cos(\gamma_{\boldsymbol{k}}t)], && \text{(A5)}\\
\alpha_{\boldsymbol{k}}\alpha_{\boldsymbol{k}}(t) &= \tfrac{1}{4}\,\mathrm{e}^{-2(\mathrm{i}\omega(\boldsymbol{k})+\gamma_{\boldsymbol{k}})t}\left[(\mathrm{e}^{\gamma_{\boldsymbol{k}}t}-1)^2\beta_{-\boldsymbol{k}}\beta_{-\boldsymbol{k}}(0) + (\mathrm{e}^{\gamma_{\boldsymbol{k}}t}+1)^2\alpha_{\boldsymbol{k}}\alpha_{\boldsymbol{k}}(0) - 2(\mathrm{e}^{2\gamma_{\boldsymbol{k}}t}-1)\alpha_{\boldsymbol{k}}\beta_{-\boldsymbol{k}}(0)\right], && \text{(A6)}\\
\beta_{\boldsymbol{k}}\beta_{\boldsymbol{k}}(t) &= \tfrac{1}{4}\,\mathrm{e}^{-2(\mathrm{i}\omega(\boldsymbol{k})+\gamma_{\boldsymbol{k}})t}\left[(\mathrm{e}^{\gamma_{\boldsymbol{k}}t}-1)^2\alpha_{-\boldsymbol{k}}\alpha_{-\boldsymbol{k}}(0) + (\mathrm{e}^{\gamma_{\boldsymbol{k}}t}+1)^2\beta_{\boldsymbol{k}}\beta_{\boldsymbol{k}}(0) - 2(\mathrm{e}^{2\gamma_{\boldsymbol{k}}t}-1)\alpha_{-\boldsymbol{k}}\beta_{\boldsymbol{k}}(0)\right], && \text{(A7)}\\
\alpha_{\boldsymbol{k}}\beta_{-\boldsymbol{k}}(t) &= \tfrac{1}{4}\,\mathrm{e}^{-2(\mathrm{i}\omega(\boldsymbol{k})+\gamma_{\boldsymbol{k}})t}\left[(\mathrm{e}^{2\gamma_{\boldsymbol{k}}t}-1)\alpha_{\boldsymbol{k}}\alpha_{\boldsymbol{k}}(0) + (\mathrm{e}^{2\gamma_{\boldsymbol{k}}t}-1)\beta_{-\boldsymbol{k}}\beta_{-\boldsymbol{k}}(0) - 2(\mathrm{e}^{2\gamma_{\boldsymbol{k}}t}+1)\alpha_{\boldsymbol{k}}\beta_{-\boldsymbol{k}}(0)\right], && \text{(A8)}\\
\alpha_{\boldsymbol{k}}\alpha^\dagger_{-\boldsymbol{k}}(t) &= \tfrac{1}{4}\,\mathrm{e}^{-2\gamma_{\boldsymbol{k}}t}\left[(\mathrm{e}^{\gamma_{\boldsymbol{k}}t}-1)^2\beta_{-\boldsymbol{k}}\beta^\dagger_{\boldsymbol{k}}(0) + (\mathrm{e}^{\gamma_{\boldsymbol{k}}t}+1)^2\alpha_{\boldsymbol{k}}\alpha^\dagger_{-\boldsymbol{k}}(0) - 2(\mathrm{e}^{2\gamma_{\boldsymbol{k}}t}-1)\alpha_{\boldsymbol{k}}\beta^\dagger_{\boldsymbol{k}}(0)\right], && \text{(A9)}\\
\beta_{-\boldsymbol{k}}\beta^\dagger_{\boldsymbol{k}}(t) &= \tfrac{1}{4}\,\mathrm{e}^{-2\gamma_{\boldsymbol{k}}t}\left[(\mathrm{e}^{\gamma_{\boldsymbol{k}}t}-1)^2\alpha_{\boldsymbol{k}}\alpha^\dagger_{-\boldsymbol{k}}(0) + (\mathrm{e}^{\gamma_{\boldsymbol{k}}t}+1)^2\beta_{-\boldsymbol{k}}\beta^\dagger_{\boldsymbol{k}}(0) - 2(\mathrm{e}^{2\gamma_{\boldsymbol{k}}t}-1)\alpha_{\boldsymbol{k}}\beta^\dagger_{\boldsymbol{k}}(0)\right], && \text{(A10)}\\
\alpha_{\boldsymbol{k}}\beta^\dagger_{\boldsymbol{k}}(t) &= \tfrac{1}{4}\left[(\mathrm{e}^{-2\gamma_{\boldsymbol{k}}t}-1)\alpha_{\boldsymbol{k}}\alpha^\dagger_{-\boldsymbol{k}}(0) + (\mathrm{e}^{-2\gamma_{\boldsymbol{k}}t}-1)\beta_{-\boldsymbol{k}}\beta^\dagger_{\boldsymbol{k}}(0) + (\mathrm{e}^{-2\gamma_{\boldsymbol{k}}t}+1)\alpha_{\boldsymbol{k}}\beta^\dagger_{\boldsymbol{k}}(0)\right], && \text{(A11)}\\
\alpha_{\boldsymbol{k}}\alpha_{-\boldsymbol{k}}(t) &= \tfrac{1}{4}\,\mathrm{e}^{-2(\mathrm{i}\omega(\boldsymbol{k})+\gamma_{\boldsymbol{k}})t}\left[(\mathrm{e}^{\gamma_{\boldsymbol{k}}t}+1)^2\alpha_{\boldsymbol{k}}\alpha_{-\boldsymbol{k}}(0) + (\mathrm{e}^{\gamma_{\boldsymbol{k}}t}-1)^2\beta_{\boldsymbol{k}}\beta_{-\boldsymbol{k}}(0) - (\mathrm{e}^{2\gamma_{\boldsymbol{k}}t}-1)(\alpha_{\boldsymbol{k}}\beta_{\boldsymbol{k}} + \alpha_{-\boldsymbol{k}}\beta_{-\boldsymbol{k}})(0)\right], && \text{(A12)}\\
\beta_{\boldsymbol{k}}\beta_{-\boldsymbol{k}}(t) &= \tfrac{1}{4}\,\mathrm{e}^{-2(\mathrm{i}\omega(\boldsymbol{k})+\gamma_{\boldsymbol{k}})t}\left[(\mathrm{e}^{\gamma_{\boldsymbol{k}}t}+1)^2\beta_{\boldsymbol{k}}\beta_{-\boldsymbol{k}}(0) + (\mathrm{e}^{\gamma_{\boldsymbol{k}}t}-1)^2\alpha_{\boldsymbol{k}}\alpha_{-\boldsymbol{k}}(0) - (\mathrm{e}^{2\gamma_{\boldsymbol{k}}t}-1)(\alpha_{\boldsymbol{k}}\beta_{\boldsymbol{k}} + \alpha_{-\boldsymbol{k}}\beta_{-\boldsymbol{k}})(0)\right], && \text{(A13)}\\
\alpha_{\boldsymbol{k}}\beta_{\boldsymbol{k}}(t) &= \tfrac{1}{4}\,\mathrm{e}^{-2(\mathrm{i}\omega(\boldsymbol{k})+\gamma_{\boldsymbol{k}})t}\left[(\mathrm{e}^{\gamma_{\boldsymbol{k}}t}+1)^2\alpha_{\boldsymbol{k}}\beta_{\boldsymbol{k}}(0) + (\mathrm{e}^{\gamma_{\boldsymbol{k}}t}-1)^2\alpha_{-\boldsymbol{k}}\beta_{-\boldsymbol{k}}(0) - (\mathrm{e}^{2\gamma_{\boldsymbol{k}}t}-1)(\alpha_{\boldsymbol{k}}\alpha_{-\boldsymbol{k}} + \beta_{\boldsymbol{k}}\beta_{-\boldsymbol{k}})(0)\right]. && \text{(A14)}
\end{aligned}$$

Appendix B: Computation of the 2-spin correlator $S_\perp(\boldsymbol{r}_1,\boldsymbol{r}_2,t)$

We can compute the evolution of $S_\perp(\boldsymbol{r}_1,\boldsymbol{r}_2)$ in the Heisenberg picture. For $a_{\boldsymbol{r}_1}a^\dagger_{\boldsymbol{r}_2}$ we have

$$\begin{aligned}
(a_{\boldsymbol{r}_1}a^\dagger_{\boldsymbol{r}_2})(t) &= \frac{1}{N_A}\sum_{\boldsymbol{k},\boldsymbol{k}'}\mathrm{e}^{-\mathrm{i}\boldsymbol{k}\cdot\boldsymbol{r}_1}\mathrm{e}^{\mathrm{i}\boldsymbol{k}'\cdot\boldsymbol{r}_2}(a_{\boldsymbol{k}}a^\dagger_{\boldsymbol{k}'})(t) && \text{(B1)}\\
&= \frac{1}{N_A}\sum_{\boldsymbol{k},\boldsymbol{k}'}\mathrm{e}^{-\mathrm{i}\boldsymbol{k}\cdot\boldsymbol{r}_1}\mathrm{e}^{\mathrm{i}\boldsymbol{k}'\cdot\boldsymbol{r}_2}\{[\cosh(\theta_{\boldsymbol{k}})\alpha_{\boldsymbol{k}} - \sinh(\theta_{\boldsymbol{k}})\beta^\dagger_{\boldsymbol{k}}][\cosh(\theta_{\boldsymbol{k}'})\alpha^\dagger_{\boldsymbol{k}'} - \sinh(\theta_{\boldsymbol{k}'})\beta_{\boldsymbol{k}'}]\}(t).
\end{aligned}$$

By using Eqs. (A1)–(A5) and simplifying the mean values which vanish on the ground state, the sum is left only with the terms where $\boldsymbol{k}=\boldsymbol{k}'$:

$$\begin{aligned}\langle a_{\boldsymbol{r}_1} a^\dagger_{\boldsymbol{r}_2}(t)\rangle &= \frac{1}{N_A}\sum_{\boldsymbol{k}} \mathrm{e}^{-\mathrm{i}\boldsymbol{k}\cdot(\boldsymbol{r}_1-\boldsymbol{r}_2)}[\cosh^2(\theta_{\boldsymbol{k}})\langle\alpha^\dagger_{\boldsymbol{k}}\alpha_{\boldsymbol{k}}(t)\rangle+\sinh^2(\theta_{\boldsymbol{k}})\langle\beta^\dagger_{\boldsymbol{k}}\beta_{\boldsymbol{k}}(t)\rangle+\cosh^2(\theta_{\boldsymbol{k}})]\\ &= \frac{1}{N_A}\sum_{\boldsymbol{k}} \mathrm{e}^{-\mathrm{i}\boldsymbol{k}\cdot(\boldsymbol{r}_1-\boldsymbol{r}_2)}\left\{\cosh(2\theta_{\boldsymbol{k}})\bar{n}_{\boldsymbol{k}}\left[1-\mathrm{e}^{-\gamma_{\boldsymbol{k}}t}\cos(\gamma_{\boldsymbol{k}}t)\right]+\cosh^2(\theta_{\boldsymbol{k}})\right\}. \end{aligned}\tag{B2}$$

Similarly, the remaining terms for $\boldsymbol{r}_2\in A$ give:

$$\begin{aligned}\langle a^\dagger_{\boldsymbol{r}_1} a_{\boldsymbol{r}_2}(t)\rangle &= \frac{1}{N_A}\sum_{\boldsymbol{k}} \mathrm{e}^{-\mathrm{i}\boldsymbol{k}\cdot(\boldsymbol{r}_2-\boldsymbol{r}_1)}[\cosh^2(\theta_{\boldsymbol{k}})\langle\alpha^\dagger_{\boldsymbol{k}}\alpha_{\boldsymbol{k}}(t)\rangle+\sinh^2(\theta_{\boldsymbol{k}})\langle\beta^\dagger_{\boldsymbol{k}}\beta_{\boldsymbol{k}}(t)\rangle+\sinh^2(\theta_{\boldsymbol{k}})]\\ &= \frac{1}{N_A}\sum_{\boldsymbol{k}} \mathrm{e}^{-\mathrm{i}\boldsymbol{k}\cdot(\boldsymbol{r}_2-\boldsymbol{r}_1)}\left\{\cosh(2\theta_{\boldsymbol{k}})\bar{n}_{\boldsymbol{k}}\left[1-\mathrm{e}^{-\gamma_{\boldsymbol{k}}t}\cos(\gamma_{\boldsymbol{k}}t)\right]+\sinh^2(\theta_{\boldsymbol{k}})\right\}, \end{aligned}\tag{B3}$$

$$\langle a_{\boldsymbol{r}_1} a_{\boldsymbol{r}_2}(t)\rangle = \langle a^\dagger_{\boldsymbol{r}_1} a^\dagger_{\boldsymbol{r}_2}(t)\rangle^* = \frac{-1}{N_A}\sum_{\boldsymbol{k}} \mathrm{e}^{-\mathrm{i}\boldsymbol{k}\cdot(\boldsymbol{r}_1-\boldsymbol{r}_2)}\sinh(2\theta_{\boldsymbol{k}})\bar{n}_{\boldsymbol{k}}\,\mathrm{e}^{-\gamma_{\boldsymbol{k}}t}\sin(\gamma_{\boldsymbol{k}}t). \tag{B4}$$

and for $\boldsymbol{r}_2\in B$:

$$\begin{aligned}\langle a_{\boldsymbol{r}_1} b_{\boldsymbol{r}_2}(t)\rangle &= \langle a^\dagger_{\boldsymbol{r}_1} b^\dagger_{\boldsymbol{r}_2}(t)\rangle^* = \frac{-1}{\sqrt{N_AN_B}}\sum_{\boldsymbol{k}} \mathrm{e}^{-\mathrm{i}\boldsymbol{k}\cdot(\boldsymbol{r}_2-\boldsymbol{r}_1)}\cosh(\theta_{\boldsymbol{k}})\sinh(\theta_{\boldsymbol{k}})[\langle\alpha^\dagger_{\boldsymbol{k}}\alpha_{\boldsymbol{k}}(t)\rangle+\langle\beta^\dagger_{\boldsymbol{k}}\beta_{\boldsymbol{k}}(t)\rangle+1]\\ &= \frac{-1}{2\sqrt{N_AN_B}}\sum_{\boldsymbol{k}} \mathrm{e}^{-\mathrm{i}\boldsymbol{k}\cdot(\boldsymbol{r}_2-\boldsymbol{r}_1)}\sinh(2\theta_{\boldsymbol{k}})\left\{2\bar{n}_{\boldsymbol{k}}\left[1-\mathrm{e}^{-\gamma_{\boldsymbol{k}}t}\cos(\gamma_{\boldsymbol{k}}t)\right]+1\right\}, \end{aligned}\tag{B5}$$

$$\langle a_{\boldsymbol{r}_1} b^\dagger_{\boldsymbol{r}_2}(t)\rangle = \langle a^\dagger_{\boldsymbol{r}_1} b_{\boldsymbol{r}_2}(t)\rangle^* = \frac{1}{\sqrt{N_AN_B}}\sum_{\boldsymbol{k}} \mathrm{e}^{-\mathrm{i}\boldsymbol{k}\cdot(\boldsymbol{r}_1-\boldsymbol{r}_2)}\cosh(2\theta_{\boldsymbol{k}})\bar{n}_{\boldsymbol{k}}\,\mathrm{e}^{-\gamma_{\boldsymbol{k}}t}\sin(\gamma_{\boldsymbol{k}}t). \tag{B6}$$

Thus, on one hand, the correlation function for $\boldsymbol{r}_2\in A$ reads

$$\begin{aligned}S_\perp(\boldsymbol{r}_1,\boldsymbol{r}_2,t) &= \frac{S}{2N_A}\sum_{\boldsymbol{k}}\cos[\boldsymbol{k}\cdot(\boldsymbol{r}_1-\boldsymbol{r}_2)]\left(\cosh(2\theta_{\boldsymbol{k}})\left\{2\bar{n}_{\boldsymbol{k}}\left[1-\mathrm{e}^{-\gamma_{\boldsymbol{k}}t}\cos(\gamma_{\boldsymbol{k}}t)\right]+1\right\}-2\sinh(2\theta_{\boldsymbol{k}})\bar{n}_{\boldsymbol{k}}\,\mathrm{e}^{-\gamma_{\boldsymbol{k}}t}\sin(\gamma_{\boldsymbol{k}}t)\right)\\ &+ \mathrm{i}\frac{S}{2N_A}\sum_{\boldsymbol{k}}\sin[\boldsymbol{k}\cdot(\boldsymbol{r}_1-\boldsymbol{r}_2)]. \end{aligned}\tag{B7}$$

Since

$$\frac{1}{N_A}\sum_{\boldsymbol{k}}\sin[\boldsymbol{k}\cdot(\boldsymbol{r}_1-\boldsymbol{r}_2)] = \mathrm{Im}\left\{\frac{1}{N_A}\sum_{\boldsymbol{k}}\mathrm{e}^{\mathrm{i}\boldsymbol{k}\cdot(\boldsymbol{r}_1-\boldsymbol{r}_2)}\right\} = \mathrm{Im}\left(\delta_{\boldsymbol{r}_1,\boldsymbol{r}_2}\right)=0, \tag{B8}$$

and using (13):

$$S_\perp(\boldsymbol{r}_1,\boldsymbol{r}_2,t) = \frac{S}{2N_A}\sum_{\boldsymbol{k}}\cos[\boldsymbol{k}\cdot(\boldsymbol{r}_1-\boldsymbol{r}_2)]\left(\frac{d+2\bar{n}_{\boldsymbol{k}}\left\{d[1-\mathrm{e}^{-\gamma_{\boldsymbol{k}}t}\cos(\gamma_{\boldsymbol{k}}t)]-\xi_{\boldsymbol{k}}\,\mathrm{e}^{-\gamma_{\boldsymbol{k}}t}\sin(\gamma_{\boldsymbol{k}}t)\right\}}{\sqrt{d^2-\xi^2_{\boldsymbol{k}}}}\right). \tag{B9}$$

And on the other hand, for $\boldsymbol{r}_2\in B$,

$$S_\perp(\boldsymbol{r}_1,\boldsymbol{r}_2,t) = \frac{-S}{2\sqrt{N_AN_B}}\sum_{\boldsymbol{k}}\cos[\boldsymbol{k}\cdot(\boldsymbol{r}_1-\boldsymbol{r}_2)]\left(\frac{\xi_{\boldsymbol{k}}+2\bar{n}_{\boldsymbol{k}}\left\{\xi_{\boldsymbol{k}}[1-\mathrm{e}^{-\gamma_{\boldsymbol{k}}t}\cos(\gamma_{\boldsymbol{k}}t)]-d\,\mathrm{e}^{-\gamma_{\boldsymbol{k}}t}\sin(\gamma_{\boldsymbol{k}}t)\right\}}{\sqrt{d^2-\xi^2_{\boldsymbol{k}}}}\right). \tag{B10}$$

[1] A. Auerbach, *Interacting Electrons and Quantum Magnetism* (Springer-Verlag, New York, 1994).

[2] J. Gonzalez, M. A. Martin-Delgado, G. Sierra and A. H.

Vozmediano, *Quantum Electron Liquids and High-Tc Superconductivity* (Lecture Notes in Physics Monographs; Springer-Verlag, New York, 1995).

[3] W. F. Brown Jr., Phys. Rev. **130**, 16771686 (1963).

[4] A. Rivas and S.F. Huelga, *Open Quantum Systems. An Introduction* (Springer, Heidelberg, 2011).

[5] U. Weiss, *Quantum Dissipative Systems* (World Scientific, Singapore, 2008).

[6] H. -P. Breuer and F. Petruccione, *The Theory of Open Quantum Systems* (Oxford University Press, Oxford, 2002).

[7] C. W. Gardiner and P. Zoller, *Quantum Noise* (Springer, Berlin, 2004).

[8] M. A. Nielsen and I. L. Chuang, *Quantum Computation and Quantum Information* (Cambridge University Press, Cambridge, 2000).

[9] A. Galindo and M. A. Martin-Delgado, Rev. Mod. Phys. **74**, 347-423, (2002); arXiv:quant-ph/0112105.

[10] G. Shirane, Y. Endoh, R. J. Birgeneau, M. A. Kastner, Y. Hidaka, M. Oda, M. Suzuki and T. Murakami, Phys. Rev. Lett. **59**, 1613–1616 (1987).

[11] G. Aeppli, S. M. Hayden, H. A. Mook, Z. Fisk, S.-W. Cheong, D. Rytz, J. P. Remeika, G. P. Espinosa and A. S. Cooper, Phys. Rev. Lett. **62**, 2052–2055 (1989).

[12] T. G. Perring, G. Aeppli, S. M. Hayden, S. A. Carter, J. P. Remeika and S-W Cheong, Phys. Rev. Lett. **77**, 711–714 (1996).

[13] K. B. Lyons, P. A. Fleury, J. P. Remeika, A. S. Cooper and T. J. Negran, Phys. Rev. B **37**, 2353–2356 (1988).

[14] E. Manousakis, Rev. Mod. Phys. **26**, 1 (1991).

[15] T. Holstein and H. Primakoff, Phys. Rev. **58**, 1098–1113 (1940).

[16] P. W. Anderson, Phys. Rev. **86**, 694–701 (1952).

[17] K. Kubo, Phys. Rev. Lett. **61**, 110 (1988).

[18] A. J. Leggett, S. Chakravarty, A. T. Dorsey, M. P. A. Fisher, A. Garg and W. Zwerger, Rev. Mod. Phys. **59**, 1 (1987).

[19] E. B. Davies, Commun. Math. Phys. **39**, 91 (1974).

[20] A. Rivas, A. D. K. Plato, S. F. Huelga and M. B. Plenio, New J. Phys. **12**, 113032 (2010).

[21] N. D. Mermin, H. Wagner, Phys. Rev. Lett. **17**, 1133–1136 (1966).